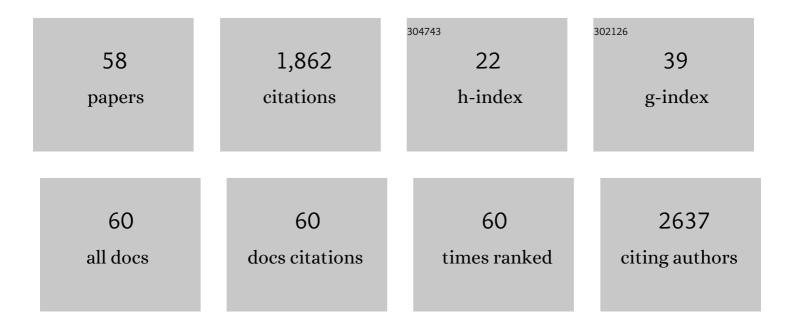
## Jeroen Siero

List of Publications by Year in descending order

Source: https://exaly.com/author-pdf/37963/publications.pdf Version: 2024-02-01



IEDOEN SIEDO

#	Article	IF	CITATIONS
1	Probabilistic tractography recovers a rostrocaudal trajectory of connectivity variability in the human insular cortex. Human Brain Mapping, 2012, 33, 2005-2034.	3.6	255
2	Ultra-high field MRI: Advancing systems neuroscience towards mesoscopic human brain function. NeuroImage, 2018, 168, 345-357.	4.2	151
3	Cortical Depth-Dependent Temporal Dynamics of the BOLD Response in the Human Brain. Journal of Cerebral Blood Flow and Metabolism, 2011, 31, 1999-2008.	4.3	118
4	BOLD matches neuronal activity at the mm scale: A combined 7T fMRI and ECoG study in human sensorimotor cortex. NeuroImage, 2014, 101, 177-184.	4.2	97
5	Magnetic Resonance Imaging of Plaque Morphology, Burden, and Distribution in Patients With Symptomatic Middle Cerebral Artery Stenosis. Stroke, 2016, 47, 1797-1802.	2.0	69
6	Investigating the non-linearity of the BOLD cerebrovascular reactivity response to targeted hypo/hypercapnia at 7T. NeuroImage, 2014, 98, 296-305.	4.2	67
7	Examining the regional and cerebral depth-dependent BOLD cerebrovascular reactivity response at 7 T. Neurolmage, 2015, 114, 239-248.	4.2	64
8	Pushing the limits of highâ€resolution functional MRI using a simple highâ€density multiâ€element coil design. NMR in Biomedicine, 2013, 26, 65-73.	2.8	62
9	High-resolution intracranial vessel wall MRI in an elderly asymptomatic population: comparison of 3T and 7T. European Radiology, 2017, 27, 1585-1595.	4.5	59
10	BOLD Consistently Matches Electrophysiology in Human Sensorimotor Cortex at Increasing Movement Rates: A Combined 7T fMRI and ECoG Study on Neurovascular Coupling. Journal of Cerebral Blood Flow and Metabolism, 2013, 33, 1448-1456.	4.3	54
11	Bolus Arrival Time and Cerebral Blood Flow Responses to Hypercarbia. Journal of Cerebral Blood Flow and Metabolism, 2014, 34, 1243-1252.	4.3	54
12	Cortical depth dependence of the BOLD initial dip and poststimulus undershoot in human visual cortex at 7 Tesla. Magnetic Resonance in Medicine, 2015, 73, 2283-2295.	3.0	52
13	BOLD Specificity and Dynamics Evaluated in Humans at 7 T: Comparing Gradient-Echo and Spin-Echo Hemodynamic Responses. PLoS ONE, 2013, 8, e54560.	2.5	49
14	Phase contrast MRI measurements of net cerebrospinal fluid flow through the cerebral aqueduct are confounded by respiration. Journal of Magnetic Resonance Imaging, 2019, 49, 433-444.	3.4	48
15	Highâ€field MRS of the human brain at short TE and TR. NMR in Biomedicine, 2011, 24, 1081-1088.	2.8	43
16	Dissociation between Neuronal Activity in Sensorimotor Cortex and Hand Movement Revealed as a Function of Movement Rate. Journal of Neuroscience, 2012, 32, 9736-9744.	3.6	39
17	The BOLD cerebrovascular reactivity response to progressive hypercapnia in young and elderly. NeuroImage, 2016, 139, 94-102.	4.2	39
18	Quantitative Intracranial Atherosclerotic Plaque Characterization at 7T MRI: An Ex Vivo Study with Histologic Validation. American Journal of Neuroradiology, 2016, 37, 802-810.	2.4	34

JEROEN SIERO

#	Article	IF	CITATIONS
19	On the transmit field inhomogeneity correction of relaxationâ€compensated amide and NOE CEST effects at 7ÂT. NMR in Biomedicine, 2017, 30, e3687.	2.8	34
20	Laminar fMRI: What can the time domain tell us?. NeuroImage, 2019, 197, 761-771.	4.2	33
21	Real-Time Decoding of Brain Responses to Visuospatial Attention Using 7T fMRI. PLoS ONE, 2011, 6, e27638.	2.5	30
22	Neuronal activation induced BOLD and CBF responses upon acetazolamide administration in patients with steno-occlusive artery disease. NeuroImage, 2015, 105, 276-285.	4.2	26
23	Vasogenic edema versus neuroplasticity as neural correlates of hippocampal volume increase following electroconvulsive therapy. Brain Stimulation, 2020, 13, 1080-1086.	1.6	25
24	Spontaneous blood oxygenation levelâ€dependent fMRI signal is modulated by behavioral state and correlates with evoked response in sensorimotor cortex: A 7.0â€T fMRI study. Human Brain Mapping, 2012, 33, 511-522.	3.6	20
25	Effect sizes of BOLD CVR, resting-state signal fluctuations and time delay measures for the assessment of hemodynamic impairment in carotid occlusion patients. NeuroImage, 2018, 179, 530-539.	4.2	20
26	Detailed view on slow sinusoidal, hemodynamic oscillations on the human brain cortex by <scp>F</scp> ourier transforming oxy/deoxy hyperspectral images. Human Brain Mapping, 2018, 39, 3558-3573.	3.6	18
27	A line through the brain: implementation of human line-scanning at 7T for ultra-high spatiotemporal resolution fMRI. Journal of Cerebral Blood Flow and Metabolism, 2021, 41, 2831-2843.	4.3	18
28	Variable impact of CSF flow suppression on quantitative 3.0T intracranial vessel wall measurements. Journal of Magnetic Resonance Imaging, 2018, 48, 1120-1128.	3.4	16
29	Can 7T MPRAGE match MP2RAGE for gray-white matter contrast?. NeuroImage, 2021, 240, 118384.	4.2	15
30	<i>In vivo</i> quantification of hyperoxic arterial blood water <i>T</i> <sub>1</sub> . NMR in Biomedicine, 2015, 28, 1518-1525.	2.8	14
31	The Cumulative Influence of Hyperoxia and Hypercapnia on Blood Oxygenation and R <sub>2</sub> <sup>*</sup> . Journal of Cerebral Blood Flow and Metabolism, 2015, 35, 2032-2042.	4.3	14
32	Quantitative T1 mapping under precisely controlled graded hyperoxia at 7T. Journal of Cerebral Blood Flow and Metabolism, 2017, 37, 1461-1469.	4.3	13
33	Vascular reactivity in small cerebral perforating arteries with 7â€T phase contrast MRI – A proof of concept study. Neurolmage, 2018, 172, 470-477.	4.2	13
34	Automated Assessment of Cerebral Arterial Perforator Function on 7T MRI. Journal of Magnetic Resonance Imaging, 2021, 53, 234-241.	3.4	13
35	Comparison of 3T Intracranial Vessel Wall MRI Sequences. American Journal of Neuroradiology, 2018, 39, 1112-1120.	2.4	12
36	Qualitative Evaluation of a High-Resolution 3D Multi-Sequence Intracranial Vessel Wall Protocol at 3 Tesla MRI. PLoS ONE, 2016, 11, e0160781.	2.5	12

JEROEN SIERO

#	Article	IF	CITATIONS
37	Contralateral improvement of cerebrovascular reactivity and TIA frequency after unilateral revascularization surgery in moyamoya vasculopathy. NeuroImage: Clinical, 2021, 30, 102684.	2.7	11
38	Tractâ€based magnetic resonance spectroscopy of the cingulum bundles at 7 T. Human Brain Mapping, 2012, 33, 1503-1511.	3.6	10
39	On the sensitivity of the diffusion MRI signal to brain activity in response to a motor cortex paradigm. Human Brain Mapping, 2019, 40, 5069-5082.	3.6	10
40	Velocity and Pulsatility Measures in the Perforating Arteries of the Basal Ganglia at 3T MRI in Reference to 7T MRI. Frontiers in Neuroscience, 2021, 15, 665480.	2.8	10
41	Imageâ€based method to measure and characterize shimâ€induced eddy current fields. Concepts in Magnetic Resonance Part A: Bridging Education and Research, 2013, 42, 245-260.	0.5	9
42	Is there any difference in Amide and NOE CEST effects between white and gray matter at 7 T?. Journal of Magnetic Resonance, 2016, 272, 82-86.	2.1	9
43	Fast CSF MRI for brain segmentation; Cross-validation by comparison with 3D T1-based brain segmentation methods. PLoS ONE, 2018, 13, e0196119.	2.5	8
44	Comparing hand movement rate dependence of cerebral blood volume and BOLD responses at 7T. NeuroImage, 2021, 226, 117623.	4.2	8
45	Zooming in on cerebral small vessel function in small vessel diseases with 7T MRI: Rationale and design of the "ZOOM@SVDs―study. Cerebral Circulation - Cognition and Behavior, 2021, 2, 100013.	0.9	8
46	A plugâ€andâ€play, lightweight, singleâ€axis gradient insert design for increasing spatiotemporal resolution in echo planar imagingâ€based brain imaging. NMR in Biomedicine, 2021, 34, e4499.	2.8	8
47	A silent gradient axis for soundless spatial encoding to enable fast and quiet brain imaging. Magnetic Resonance in Medicine, 2022, 87, 1062-1073.	3.0	8
48	Arterial CO2 pressure changes during hypercapnia are associated with changes in brain parenchymal volume. European Radiology Experimental, 2020, 4, 17.	3.4	8
49	Hemodynamic and metabolic changes during hypercapnia with normoxia and hyperoxia using pCASL and TRUST MRI in healthy adults. Journal of Cerebral Blood Flow and Metabolism, 2022, 42, 861-875.	4.3	8
50	Comparing BOLD and VASO-CBV population receptive field estimates in human visual cortex. NeuroImage, 2022, 248, 118868.	4.2	8
51	Blood Oxygenation Level–dependent/Functional Magnetic Resonance Imaging. PET Clinics, 2013, 8, 329-344.	3.0	7
52	Establishing upper limits on neuronal activity–evoked pH changes with APT EST MRI at 7 T. Magnetic Resonance in Medicine, 2018, 80, 126-136.	3.0	7
53	Cerebrovascular Reactivity during Prolonged Breath-Hold in Experienced Freedivers. American Journal of Neuroradiology, 2018, 39, 1839-1847.	2.4	7
54	Accelerating Brain Imaging Using a Silent Spatial Encoding Axis. Magnetic Resonance in Medicine, 2022, 88, 1785-1793.	3.0	5

JEROEN SIERO

#	Article	IF	CITATIONS
55	fMRI based BCI control using spatial visual attention at 7T. , 2009, , .		4
56	Double delay alternating with nutation for tailored excitation facilitates bandingâ€free isotropic highâ€resolution intracranial vessel wall imaging. NMR in Biomedicine, 2021, 34, e4567.	2.8	3
57	Shape and volume changes of the superior lateral ventricle after electroconvulsive therapy measured with ultra-high field MRI. Psychiatry Research - Neuroimaging, 2021, 317, 111384.	1.8	1
58	No Signs of Edema or Angiogenesis in the Hippocampus After Electroconvulsive Therapy. Biological Psychiatry, 2020, 87, S426.	1.3	0